FILTRATION OF RAREFIED GAS THROUGH POROUS BODIES

P. A. Novikov and V. A. Eremenko

UDC 532.546

The filtration of a rarefied gas through porous bodies of various structures, porosities, and geometries was studied under various flow modes with the Knudsen number ranging from 10^{-4} to 2.5.

Problems concerning the filtration of a rarefied gas through porous materials are of definite theoretical and practical interest for the study of evaporation cooling and porous cooling under vacuum, for the study of sublimation drying of capillary-porous materials, etc.

In analyzing the filtration of a rarefied gas through porous materials one distinguishes between viscous, viscous-sliding, and molecular flow (in the case of high-porosity bodies, the authors of [7] considered pseudomolecular or quasi-Knudsenian flow). The difference between these modes is based on the nature of interaction between gas molecules as well as between them and the pore walls.

It is to be noted that, inasmuch as the mechanism of interaction between rarefied gas molecules and pore walls with an intricate geometry has not yet been sufficiently well explored, it becomes quite difficult to derive a single theoretical relation for the flow of a rarefied gas within the transition range of pressures, where the likelihood of viscous or molecular flow modes is the same and where, under certain conditions, both modes may coexist.

In the case of isothermal viscous flow, the quantity of gas G passing through a porous body is usually determined according to Darcy's law [1-4]. In the case of molecular flow, G is estimated quantitatively according to Knudsen's law.

The object of this study was the least explored mode of rarefied gas flow through porous bodies, namely the transition mode. Nonuniformity is the basic feature of this mode.

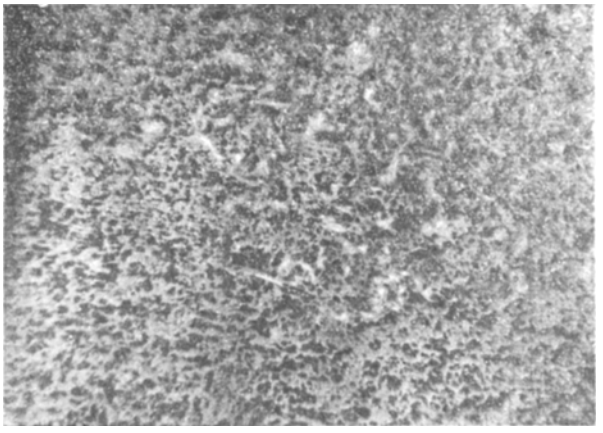

Fig. 1. Section through porous titanium (magnified 120 times).

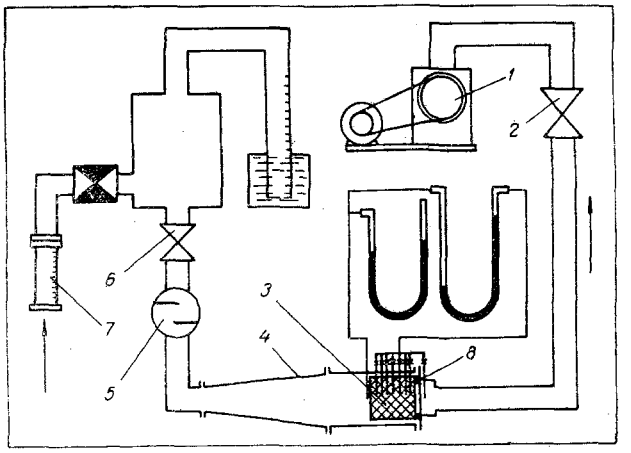

Fig. 2. Schematic diagram of the test apparatus.

Institute of Heat and Mass Transfer, Academy of Sciences of the Byelorussian SSR, Minsk. Translated from Inzhenerno-Fizicheskii Zhurnal, Vol. 23, No. 5, pp. 820-828, November, 1972. Original article submitted February 4, 1972.

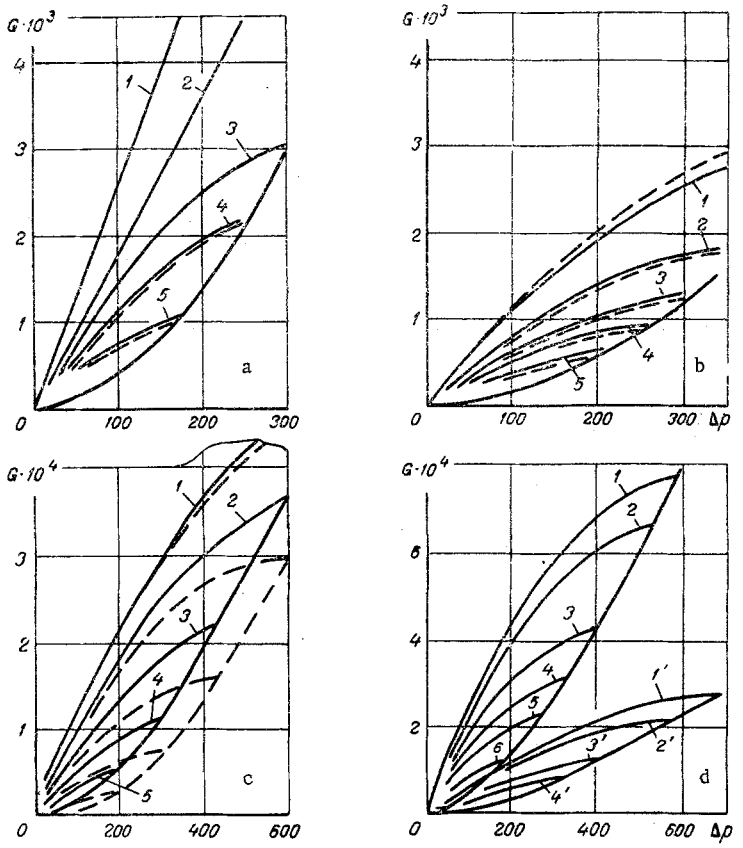

Fig. 3. Mass flow rate of rarefied gas filtering through a porous specimen, as a function of the pressure drop (Δp, mm Hg) across the specimen, based on tests at various entrance pressure levels (p_1) for (a) the model porous body consisting of glass balls 200 μm in diameter: p_1 = 600 mm Hg (1), 440 mm Hg (2), 360 mm Hg (3), 300 mm Hg (4), 200 mm Hg (5); for (b) porous titanium ($d_{eff} = 10.1 \cdot 10^{-6}$ m): p_1 = 600 mm Hg (1), 440 mm Hg (2), 360 mm Hg (3), 300 mm Hg(4), 240 mm Hg(5); for (c) porous titanium ($d_{eff} = 3.74 \cdot 10^{-6}$ m): p_1 = 747 mm Hg (1), 600 mm Hg (2), 440 mm Hg (3), 300 mm Hg (4), 200 mm Hg (5); for (d) porous graphite δ = 4.5 mm thick (curves 1-6) and δ = 21 mm thick (curves 1'-4'): p_1 = 730 mm Hg (1), 600 mm Hg (2), 440 mm Hg (3), 360 mm Hg (4), 300 mm Hg (5), 200 mm Hg (6). Solid lines represent test curves, dashed lines represent theoretical curves.

Indeed, real porous bodies (Fig. 1) contain pores of various sizes (ranging from macro to micro) and the flow of a gas through such porous bodies may be regarded as the sum of individual small streams. The overall flow characteristics depend on the relative contributions of the flow modes in those individual streams along each pore. For this reason, the flow of rarefied gas through a porous body can be analyzed by a comparison of the mass rates here and in a well known viscous flow, the latter stringently obeying Darcy's law.

In the test apparatus shown schematically in Fig. 2, rarefied air was sucked through porous bodies at a definite velocity and at definite pressure drops. The air for the filtration tests was taken in from the atmosphere by means of a model VN-4G vacuum pump 1. The air was passed through filter 5 for mechanical purification and through diffuser 4 to the active porous specimen 3.

The porous body, sealed with a rubber O-ring 8, separated the region of higher pressure from the region of lower pressure. The flow rate and the pressure of air entering the porous body were regulated by means of a vacuum check valve 2 and a needle throttle 6. The pressure of air at the entrance to the

TABLE 1. Characteristics of Porous Test Specimens

Porous specimen	Permeability $k \cdot 10^{12}$, m^2	Porosity, %	Characteristic dimension, $d_{eff} \cdot 10^6$, m	Specimen geometry		$k \cdot 10^{-4}$, N/m^2
				thickness, mm	diameter, mm	
Titanium	0,734	23	10,1	2,6	90	0,266
"	0,149	34,2	3 74	6,0	90	1,13
"	0,195	31,4	4,46	3,2	90	0,42
"	0,0356	26,4	2,08	5,4	90	1,6
Aluminum	0,795	30,8	9,1	2,8	90	0,26
Aluminum	0,237	28	5,8	2,9	90	0,73
Stainless steel	1,15	28,4	11,4	3,1	90	0,2
Graphite	0,303	47,5	4,54	4,5	80	1,33
"	0,319	47,5	4,64	7,9	80	1,33
"	0,341	47,5	4,8	10,9	80	1,33
"	0,403	47,5	5,21	21	80	1,33
Model consisting of glass balls 1000 μm in diameter	442	40	1000	11	90	10
Model consisting of glass balls 200 μm in diameter	8,0	40	200	11	90	10
Fireclay ceramics	0,01875	36,6	1,28	12,5	90	—

porous body as well as the pressure drop across the body, as a function of the entrance pressure, were measured with a vacuometer, with a differential mercury manometer, and with a differential oil manometer. The air filtration rate was measured with model RS-5 rotameters (high flow rates) 7, by the volumetric method [9], and with a model GSB-400 laboratory drum-type gas meter (low flow rates). The use of several instruments for measuring the air flow rate ensured reliable readings and the possibility of checking the results within the overlapping ranges by a comparison. The tests were performed with specimens of various porosities and structures, at a room temperature about 18°C and under an entrance pressure ranging from 40 to 760 mm Hg.

Each test series was performed over a wide range of pressure drops, under certain definite entrance pressure levels. The basic parameters of the test specimens are given in Table 1.

We estimated the error of our permeability measurements. This error was mainly due to instrument inaccuracy. According to the estimate of all components, the maximum relative error in the permeability measurement was 6%.

The mass flow rate of filtering rarefied air, as a function of the pressure drop across the specimen has been plotted from measurements and is shown in Fig. 3 by solid lines. This relation is represented here by a family of curves, each corresponding to a definite constant entrance pressure. For comparison with the test data, dashed lines are also shown here which represent calculations according to the Darcy equation. These curves are based on a constant permeability, the latter having been determined from tests with atmospheric pressure before a porous specimen and with small pressure drops across it. The deviation of test points from the theoretical curves based on Darcy's law gives an indication about the flow mode. At near atmospheric pressures before the porous body, according to Fig. 3b, c, test values can deviate from calculated values in both directions. A lower mass flow rate can be explained here by higher inertia losses [5, 6], while a higher mass flow rate can be explained by a sliding motion of gas along pore surfaces. As the entrance pressure before a porous specimen is decreased ($p_1 < 600$ mm Hg), the test points deviate from calculated values only toward higher mass flow rates. The magnitude of deviations depends on the pressure range and, according to an analysis of test data, on some characteristic dimension of the porous body.

As this characteristic dimension we have selected

$$d_{\text{eff}} = 4\sqrt{\frac{2k}{m}},$$

where k denotes the permeability of the porous body, determined from tests during a stringently viscous flow of gas in accordance with Darcy's law. (The expressions for λ and Re in [3] are also based on the characteristic dimension $d_{\text{eff}} = 4\sqrt{2k/m}$. Furthermore, the graph representing the various modes of gas flow through various porous media indicates that all points of the $\lambda = f(\text{Re})$ curve for specimens, regardless of their porosity and permeability, lie on the same straight line when plotted in logarithmic coordinates, if Darcy's law is obeyed.)

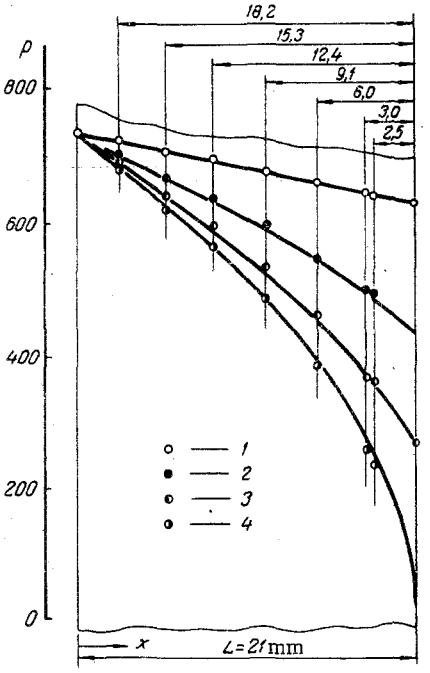

Fig. 4. Pressure profile across the specimen thickness: pressure drop 102 mm Hg (1), 470 mm Hg (2), 300 mm Hg (3), 705 mm Hg (4), calculated values (solid line). Pressure p (mm Hg).

Such a definition of the characteristic dimension is the most valid one, because it expresses the macroscopical properties of the porous body in terms of statistical quantities determined by tests.

The parameter d_{eff}, defined in terms of porosity and permeability, represents the entire size and shape spectrum of pores which make up the complex and random oriented system of channels.

For the granular model bodies composed of glass balls 1000 μm and 200 μm in diameter respectively the test curves almost coincide with the theoretical one (Fig. 3a). For porous titanium, stainless steel, and aluminum with the characteristic dimension $d_{eff} \simeq 10^{-5}$ m the test curves deviate only slightly from the theoretical ones, which can be explained by a partial departure from a purely viscous flow mode. At a gas entrance pressure of only $p_1 = 100$ mm Hg the measured mass flow rate is not more than 30% higher. For porous bodies with $d_{eff} \leq 5 \cdot 10^{-6}$ m (porous titanium, aluminum, graphite) the test curves deviate appreciably from the theoretical ones, with the measured mass flow rate more than twice as high as the mass flow rate calculated for the same entrance pressure ($p_1 = 100$ mm Hg). This can only be attributed to a change of the flow mode.

In order to explain the pressure variation across the thickness of a porous specimen and the related changes of flow modes, the authors performed an experiment with a porous graphite specimen of the same structure but of an adjustable thickness (Table 1). The pressure profile was measured in the $\delta = 21$ mm thick specimen. Into seven holes across the specimen thickness, drilled approximately 25 mm deep at definite distances from the end face (Fig. 4), were installed injection needles 1.0 mm in outside diameter. The entrance pressure before the specimen was atmospheric, the exit pressure behind the specimen was varied by means of the vacuum valve 2 shown in Fig. 2.

The test data on the pressure profile across the specimen thickness are shown in Fig. 4. This profile seems to be a parabolic one [8].

Corresponding to a parabolic pressure profile across the thickness of a porous specimen, the mean-integral pressure can be expressed as

$$\overline{p}_i = \frac{2\left(p_1^3 - p_2^3\right)}{3\left(p_1^2 - p_2^2\right)}.$$

It must be noted that, as $p_2 \to 0$, the maximum difference between the integral mean and the arithmetic mean pressure reaches approximately 33%.

These data on the pressure profile were checked against the relation $G = f(\Delta p)$ (Fig. 3d) which had been established experimentally for the 21 mm thick and for the 4.5 mm thick porous graphite specimens as follows. The maximum mass flow rate through the 21 mm specimen was $G = 2.8 \cdot 10^{-4}$ kg/sec, while the limiting pressures across the specimen thickness were as indicated in Fig. 4 by the bottom curve.

According to the profile curve, an entrance pressure of 325 mm Hg is required to ensure the same mass flow rate through the 4.5 mm specimen at the same exit pressure. Indeed, the G = f(Δp) test curve for the 4.5 mm specimen confirms this.

The pressure profile curve indicates also that, in order to ensure the same mass flow rate through specimens of various thicknesses at the same entrance pressure, the pressure drop must be large and, consequently, the relative significance of gas sliding along the exit segments of pores must increase. This, for instance, explains why the permeability of a porous specimen increases with increasing specimen thickness, as has been revealed in an analysis of the test data.

This increase in the permeability of a porous body passing a rarefied gas can be interpreted physically as follows. While flowing near a wall, a rarefied gas does not completely adhere to it ($v_W \neq 0$) but has a finite velocity: the gas slides along the surface. The sliding velocity v_s can be determined according to the equation

$$v_s = \sigma \bar{l} \frac{du}{dy}.$$

Considering that $\bar{l} \sim 1/p$ under isothermal conditions and that, to the first approximation, the transverse velocity gradient is proportional to u_0/d, we can write for the sliding velocity

$$v_s = \xi \frac{u_0}{pd},$$

where u_0 denotes the mean gas velocity without sliding in a pore of diameter d and ξ is a proportionality factor. A finite gas velocity at the wall has the effect of making the mean gas velocity in a pore higher at the same pressure drop, namely

$$u = u_0 + \Delta u,$$

where Δu denotes the increment of the mean gas velocity in a pore due to sliding. It is logical to assume that $\Delta u \sim v_s$ and then to write

$$u = u_0 + \chi \frac{u_0}{pd}.$$

Multiplying both sides of this expression by the gas density, and considering the integral nature of the gas flow through a porous body, we obtain

$$G = G_0 \left(1 + \frac{k}{\bar{p}}\right), \tag{1}$$

where coefficient k depends on the length of the characteristic dimension, on the surface structure, and on the pore shape. The values of k have been established experimentally for the porous test materials and are also given in Table 1. Here G_0 denotes the mass flow rate without sliding. The Darcy equation combined with expression (1) yields

$$G = \frac{FM}{2\mu RTL} k \left(1 + \frac{k}{\bar{p}}\right)(p_1^2 - p_2^2). \tag{2}$$

It follows from Eq. (2) that the effect of a higher mass flow rate due to sliding along pore walls becomes more significant as the mean-integral pressure decreases. This increase cannot be unlimited, however. The free path length $\bar{l}$ serves here as a limiting factor, which increases with decreasing pressure but cannot exceed d_{eff}. (The free path length must be determined by the mean-integral pressure.) The increment of mass flow rate will be maximum, therefore, when $\bar{l} = d_{eff}$. As the pressure is decreased further, $1 + k/\bar{p}$ becomes constant. At the same time, however, during rarefaction with Kn > 1 the viscosity, until now independent of the pressure [10], will become proportional to the pressure: $\mu \sim p$. In view of this, Eq. (2) can now be written as

$$G = \frac{FMk\left(1 + \frac{k}{\bar{p}}\right)}{2\mu RTL}(p_1^2 - p_2^2) = \frac{FMA}{2RTL\chi\bar{p}}(p_1^2 - p_2^2), \tag{3}$$

where $A = 1 + k/\bar{p} = \text{const}$ and $\mu = \chi p$, χ being a proportionality factor. Equation (3) reduces to

$$G = \frac{FMA}{RTL\chi}\Delta p.$$

We thus arrive at the Knudsen equation, which characterizes molecular flow when the mass flow rate does not depend on the gas density but is determined by the pressure drop alone.

The general law of gas flow through a porous body in all possible modes is

$$\frac{p_1^2 - p_2^2}{L} = \frac{2\mu RTG}{MFk\left(1 + \frac{k}{\overline{p}}\right)} + \beta\frac{G^2}{F^2},$$

where the term $\beta(G^2/F^2)$ accounts for inertia losses during filtration.

We note, in conclusion, that:

I. for viscous flow with predominant inertia losses

$$\mu = \text{const}; \left(1 + \frac{k}{\overline{p}}\right) \simeq 1; \beta = \text{const}.$$

II. for viscous flow according to Darcy's law

$$\mu = \text{const}; \left(1 + \frac{k}{\overline{p}}\right) \simeq 1; \beta = 0.$$

III. for viscous flow with sliding

$$\mu = \text{const}; \left(1 + \frac{k}{\overline{p}}\right) = \text{var}; \beta = 0.$$

IV. for molecular flow

$$\mu = \text{var}; \left(1 + \frac{k}{\overline{p}}\right) = \text{const}; \beta = 0.$$

This analysis of various modes of gas flow through porous specimens shows that a transition from one flow mode to another under changing conditions occurs smoothly. This is explained by the coexistence of the various modes across a specimen section as well as across the specimen thickness.

NOTATION

k	is the permeability, m^2;
m	is the porosity;
F	is the surface area of porous specimen, m^2;
M	is the molecular weight of gas, kg/mole;
μ	is the dynamic viscosity of gas, $N \cdot sec/m^2$;
L	is the thickness of porous specimen, m;
$R = 8.31 \cdot 10^3$ N·m/kmole·°K	is the universal gas constant;
T	is the temperature, °K;
p_1	is the entrance pressure before the porous specimen, N/m^2;
p_2	is the exit pressure behind the porous specimen, N/m^2;
v_e	is the filtration velocity, m/sec;
ρ	is the gas density, kg/m^3;
α	is the viscous drag coefficient, m^2;
β	is the inertial drag coefficient;
λ	is the hydraulic drag coefficient;
Re	is the Reynolds number.

LITERATURE CITED

1. L. S. Leibenzon, Flow of Natural Liquids and Gases through a Porous Medium [in Russian], Gostekhizdat (1947).
2. A. V. Lykov, Theoretical Principles of Structural Thermophysics [in Russian], Izd. Akad. Nauk ByelSSR, Minsk (1961).
3. G. F. Trebin, Filtration of Liquids and Gases through Porous Media [in Russian], Gostoptekhizdat (1959).
4. R. Collins, Fluid Flow through Porous Materials [Russian translation], Izd. Mir (1964).

5. E. M. Minskii, "On turbulent filtration through porous media," Dokl. Akad. Nauk SSSR, 78, No. 3 (1951).
6. I. A. Charnyi, Subterranean Hydrogasdynamics [in Russian], Gostoptekhizdat (1963).
7. B. V. Deryagin and S. P. Bakanov, Dokl. Akad. Nauk SSSR, 115, 167 (1957).
8. V. M. Aravin and S. N. Numerov, Theory of Liquid and Gas Flow through a Nondeformable Porous Medium [in Russian] (1953).
9. S. I. Kosterin, Yu. A. Koshmarov, and Yu. V. Osipov, in: Heat and Mass Transfer [in Russian], Izd. Énergiya (1963).
10. L. D. Landau and E. M. Lifshits, Mechanics of Continuous Media [in Russian], Gostekhizdat (1944).